*Ali Coşkun* ✉
*Ayhan Etyemez*
*Mustafa Ay*
*Mustafa Kurt*
*Şükran Katmer*
*Ulvi Şeker*
*Mine Nohuz*

https://doi.org/10.21278/TOF.491065024
ISSN 1333-1124
eISSN 1849-1391

# INVESTIGATION OF THE EFFECT OF THE CUTTING PARAMETERS ON CUTTING FORCES AND TOOL WEAR IN THE STACK DRILLING OF A CARBON FIBRE-REINFORCED THERMOPLASTIC MATRIX COMPOSITE AND AA7075

**Summary**

This study investigate the stack drillability of unidirectional (UD) carbon fibre reinforced thermoplastic matrix PAEK/CF composite and AA7075 plate utilised in aerospace. The effects of the cutting parameters on cutting forces during the drilling process of thermoplastic matrix composites and aluminium materials were experimentally analysed. Drilling operations were carried out on a CNC Vertical Machining Centre under dry-cutting conditions. For three different drill types, three different cutting speeds, and feed rate combinations, a total of 810 holes were drilled in a full factorial experimental design with 30 replicates for each combination. The damage on the hole surfaces on the drilled composite was identified with an optical microscope. The numerical data were obtained in the composite testing laboratory and analysed using Minitab® 21.1 statistical software and transformed into graphs. The most suitable drill type and cutting parameters were determined for the drillability of composite with thermoplastic matrix and aluminium (AA7075) plates when stacked.

*Key words:* *aeronautical thermoplastics, analysis of variance, AA7075, cutting parameters, drillability, tool wear*

## 1. Introduction

A composite is a novel material formed by combining two or more different materials at the macro level to combine the best properties of two or more different materials into a single one. In other words, these materials are composed of different types of materials or phases that are brought together to improve each other's deficiencies and obtain superior qualities. Composite materials consist of two basic components: a matrix and a reinforcement. Of these, the matrix phase forms the main component. Its main function is to wrap around the reinforcing component and hold it together in the desired form. The matrix is intended to hold the reinforcement phase together while maintaining the designed material form and to transmit and distribute any applied force to the reinforcement phase through the interfacial bond without being destroyed. Matrix materials can be composed of metal, ceramic, or polymer materials depending on the intended use and production method of the composite material.

In the aerospace manufacturing industry, aircraft structural materials with a high strength-to-weight ratio, low cost, and short processing time are preferred [1]. Here, drilling is the most widely used manufacturing process among other machining processes. The riveting process is one of the assembly processes used extensively in this industry. In this context, aerospace drilling is an integral part of rivet assembly. There are approximately 85,000 rivets in an aircraft deemed to be medium-sized.

The aerospace industry is among the sectors most affected by advances in materials science. Along with rising fuel costs, operating and maintenance costs have fuelled the search for "more lightness", as reducing the fuselage weight of airplanes leads to lower fuel consumption, reducing carbon emissions and operating costs [2]. At this point, thermoplastic composite materials are the remedy for the industry's demand for more lightness without compromising safety. The advantages include invisibility, the formation of complex aerodynamic shapes with metals, and the simplification of the assembly process by reducing the number of parts. The disadvantages include the high cost of delamination as it is a new material, the high cost of production as it is usually a labour-intensive and complex process, and the fact that delamination and cracks in composite materials are mostly intrinsic and therefore require complex inspection techniques and damage inspection.

Thermoplastics are polymers formed by molecules with linear and flexible branched-chain bonds that interact through Van Der Waals forces. They can be amorphous or crystalline and can soften or harden with heat. Those that initially soften when the temperature is increased transform into liquid form when the temperature continues to rise [3]. The increase in temperature accelerates the molecular motion, causing the Van der Waals bonds to weaken and break. This leads first to softening and then to liquefaction. Hardening occurs when the cooling process is carried out. The process involving heating and cooling is repeatable and reversible for thermoplastics. However, if the process of heating reaches extremely high temperatures, thermoplastics are subject to irreversible degradation. During the manufacturing process, the forming process is also carried out by utilising the characteristics of temperature and softening [4].

Concerning the drilling of composite materials, in their study "Thermo-Mechanical and Delamination Properties in Drilling GFRP Composites by Various Drill Angles", Usama et al. investigated the thermo-mechanical and delamination properties of GFRP (Glass Fibre Reinforced Plastics) composites in drilling holes with various drill angles. The aim of the study was to experimentally investigate the effects of drilling factors on the thermal-mechanical properties and delamination during the drilling of GFRP composite materials. In the drilling process, three different drill bit angles were applied to the CNC Vertical Machining Centre under dry cutting conditions with a drill bit of a certain diameter. In the analysis, drill spindle speed was applied at three different rpm, three different feed rates, and three different sample thicknesses. The thrust force/torque through drilling was measured using a dynamometer, and the pull-in and push-out delamination was evaluated based on the image analysed with an AutoCAD tool. In another study on the drilling of composites, it was found that all machining parameters had a significant effect on the measured temperature, where the layer thickness had the largest contribution (33.14%), followed by the drill spindle speed and feed rate (29.00% and 15.10% respectively), while the drill bit angle had the lowest contribution (11.85%) [5].

Considering the use of thermoplastic composite materials in aircraft structures, their first application was on the rudder section of the A330-200 model of the Airbus. Due to the high strength-to-weight ratio and chemical resistance, recently developed thermoplastic matrices have been used. Today, according to Airbus, there are approximately 1,400 thermoplastic composite parts on each Airbus 340-500 and 340-600 aircraft. Thermoplastic matrix composite materials contribute greatly to the formation of overly complex shapes with a very smooth surface. Along with the structural advantages, the use of thermoplastic composites also contributes to the improvement of passenger comfort. Utilising this material reduces operating costs by around 20% through reduced weight, offering a larger capacity or larger seating area. A significant amount of thermoplastic composite material parts are planned to be used in the Airbus 380 aircraft structure, including the leading edge of the wing, the vertical stabiliser, elevators, lower floor beams, the leading edge of the vertical stabiliser, upper-level floor beams, outer flaps, ailerons, the main stairs, the cockpit access stairs, the unpressurised nose section, fuselage panels, window frames, side wall and floor panels, cargo bins, elbows, cable fasteners, and the bulk cargo compartment. Composite materials are also used in military aircraft such as the B-1, F-14, F-15, and F-16 to reduce the structural weight of the aircraft. In these aircraft, composite components are used in the horizontal and vertical stabilisers, wing coverings, fixed rudder boxes, flaps, and other structural components. The mass reduction achieved in the above components generally ranges between 20% and 35%, with the main gains in fighter aircraft achieved through increased payload capacity and missile range [6]. Fig. 1 shows the change in the use of composite materials in the field of aerospace over the years, and Fig. 2 shows where composite parts and the aircraft engine are used in the F35 A fighter aircraft.

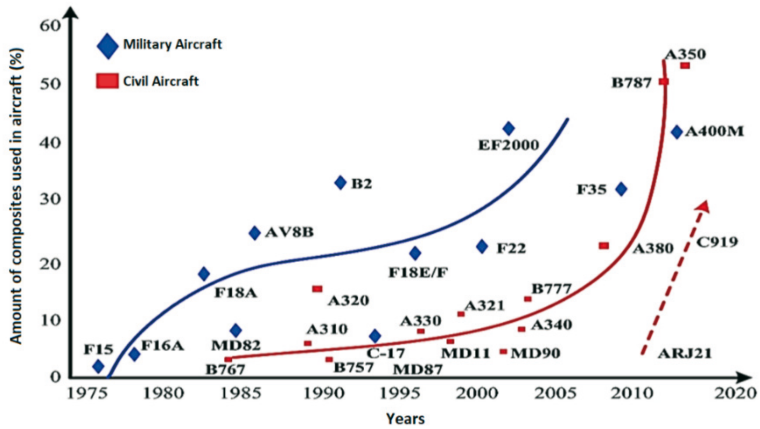


**Fig. 1** Usage rates of composite materials in aircraft structures by years [7]

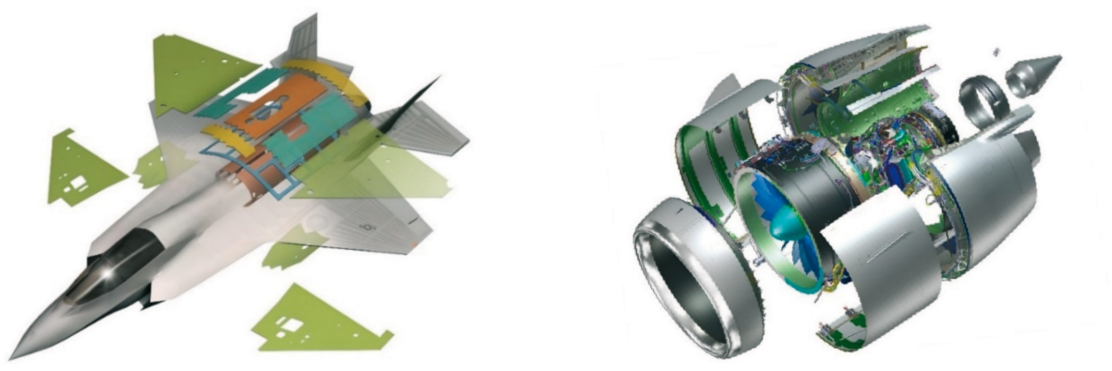

(a) (b)

**Fig. 2** (a) Some composite parts used in the F-35A fighter fuselage [7];
(b) Some composite parts used in the aircraft engine [8]

Regarding the drilling of thermoplastics, in "Drilling of Long Fiber Reinforced Thermoplastics – The Influence of the Cutting Edge on The Machining Results" by Vikki Franke, the cutting edge has a great influence on the performance of the cutting tool when drilling fibre-reinforced composites. Delamination, burrs, and defects at the hole entry and exit pose a challenge when drilling. The study investigated the effect of the cutting edge on hole quality in the machining of long fibre-reinforced thermoplastics. The effect of the cutting parameters on the machining results of the cutting edge was also investigated and the effect of the cutting edge on the hole quality on the machining results was determined. It was stated that the increase in feed force would lead to a decrease in hole quality and that, contrary to the current understanding of metal drilling, the high quality required when drilling fibre can only be achieved with sharp cutting edges. [9].

Guided by the information above, this article aims to examine through stack drilling tests the numerical data of cutting forces and tool wear of thermoplastic matrix composite material (Toray Cetex TC 1225) and aluminium AA7075, which have been widely used in aerospace. The study investigates the percentage effect of the cutting parameters on the cutting force with a combination of three different drill types, three different cutting speeds, and three different feed rates, and determines the drill type that produces the best drilling performance with the least tool wear among the three different drill types based on the forces used.

## 2. Material and method

### 2.1 Thermoplastic matrix composite material

This study experimentally investigated the stack drilling of PAEK/CF composite sheets with AA7075, the geometry of which is given in Fig. 3. For the drilling experiments, a total of 810 holes, 30 holes for each of 27 different drilling experiments in different combinations of three different types of drills, three different cutting speeds (55 m/min, 95 m/min, 165 m/min), and three different feed rate (0.1 mm/rev, 0.2 mm/rev, 0.3 mm/rev) combinations of PEEK (Polyether Ether Ketone) thermoplastic matrix composite and aluminium (AA7075) stack structures from the Poly Aryl Ether Ketone (PAEK) family, the dimensions of which are given below, were drilled with a CNC Vertical Machining Centre under dry cutting conditions. An optical microscope was used to visualise the hole damage on the surface machined by the cutting edge of the drill for this thermoplastic composite material (Toray Cetex® TC1225) that was subjected to the drilling test. To determine the percentage effect of the cutting parameters on the cutting force and the type of drill with the least tool wear and the best drilling performance among the three different drill types based on the forces applied, the data were analysed by an analysis of variance with a full factorial experimental design using Minitab® 21.1 Statistical Software.

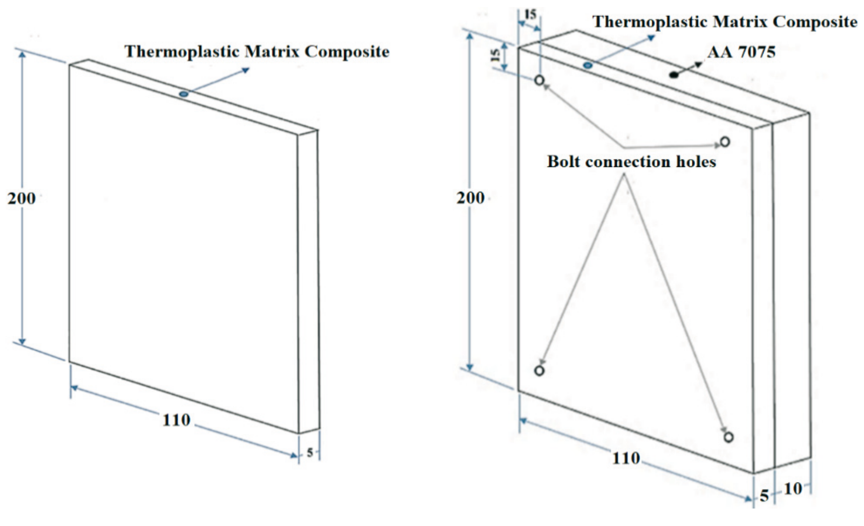


**Fig. 3** Thermoplastic matrix composite and aluminium (AA7075) stack

In this article, nine PEEK Thermoplastic Matrix Composite / PEEK - Toray Cetex® TC1225 of 200 x 110 x 5 mm and nine aluminium (AA7075) plates of 200 x 110 x 10 mm, the appearance and geometry of which are given in Fig. 4, were used as stacks. Table 1 shows the physical properties of the Toray Cetex® PEEK thermoplastic matrix composite.

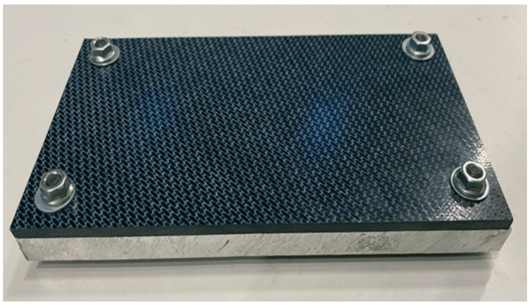

(a)

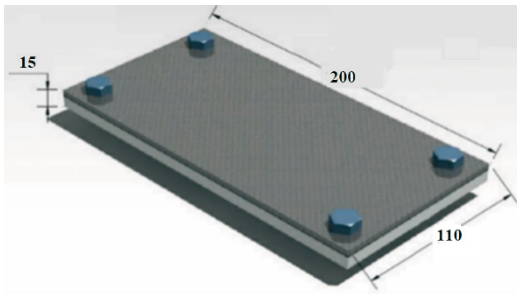


(b)

**Fig. 4** (a) Stack view of the thermoplastic matrix composite and AA7075 plates; (b) stack sample geometry

**Table 1** PAEK/CF Thermoplastic matrix composite material properties [10]

| | |
|---|---|
| Maximum Operating Temperature | 130 °C |
| Machining Temperature | 320 °C - 380 °C |
| $T_g$ Glass Transition Temperature | 147 °C |
| $T_m$ Melting Temperature | 305 °C |
| $T_c$ Crystallisation Temperature | 263 °C |
| Density | 1.59 g/cm³ |
| Weight of each Layer (Prepreg) | 221 g/m² |
| Resin Ratio by Weight | %34 |
| Layer (Prepreg) Thickness | 0.14 mm |

The PAEK/CF thermoplastic matrix composite material, the properties of which are given in Table 1, is used in light aircraft wing leading edges for its structural properties and impact resistance. This material, epoxy adhesives, and composite surfacing films are commercially available with and without lightning strike protection. It is also used in aircraft interiors as it has high impact resistance, flame retardancy, and low moisture retention properties. It is also a high-end thermoplastic composite material that utilises PAEK resin with a semi-crystalline structure combined with excellent mechanical and thermal performance. The PEEK Thermoplastic matrix composite (Toray Cetex® TC1225) is characterised by superior machinability due to its low melt viscosity, relatively low processing temperature, reduced energy consumption resulting from shorter cycle times, excellent mechanical performance at elevated temperatures, excellent toughness and compression resistance after impact, very low moisture absorption, and superior chemical solvent resistance. It is used in primary and secondary aircraft structures and hypersonic aircraft, jet engines and non-rotating fixed parts, rocket engine nozzles, etc. Overall, global demand for aircraft has been on the rise and the aerospace industry requires composites to reduce weight, improve manufacturing times, and cut costs [11].

## 2.2 Aluminium (AA7075)

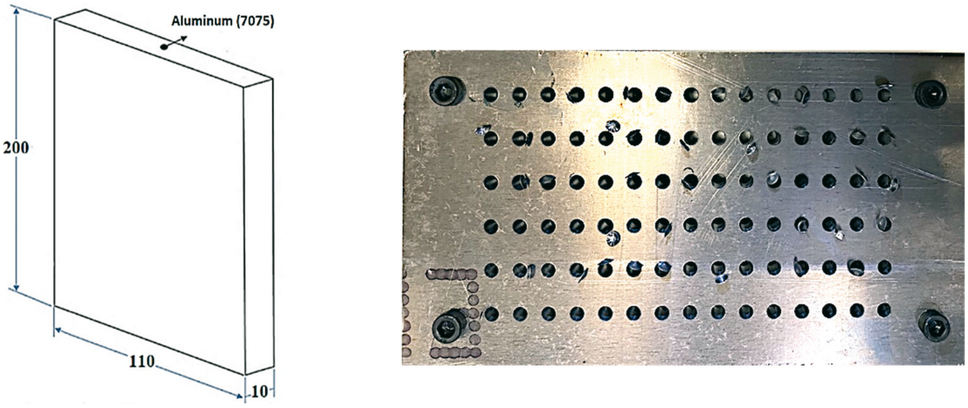


**Fig. 5** Geometry and sample view of an AA7075 plate

The main constituent elements of the aluminium (AA7075) alloy, the geometry and sample view of which are given in Fig. 5 for the AA7075 plate, are zinc, magnesium, and copper. AA7075 is characterised by its high strength, hardness, high wear resistance, and easy machinability. This material is widely preferred in high-tensile construction materials and is widely used in the aerospace, mould manufacturing, and defence industries. AA7075 is preferred over steel in many areas for its high strength, suitability for thermal processing, and lighter weight. However, the material's corrosion resistance and weldability are quite low compared to other alloy series, due to its copper and zinc content. The physical and mechanical properties and the thermal and alloy properties are given in Table 2. In the aerospace industry, AA7075 is used in many structural materials of aircraft. In particular, AA7075-T6 and AA7075-T651 aluminium plates and sheets are used in aircraft wings, seats, flaps, landing gear, the main fuselage and beams, hydraulic systems, connection rivets, and engine outlet sections [12].

**Table 2** Aluminium (Al 7075) properties [13]

| Physical and Mechanical Properties | | Thermal and Alloy Properties | |
|---|---|---|---|
| Density (ρ) | 2.81 g/cm³ | Melting temperature ($T_m$) | 477 °C |
| Young's modulus (E) | 71.7 GPa | Thermal Conductivity (k) | 130–150 W/m*K |
| Ultimate tensile strength (σt) | 572 MPa | Coefficient of thermal expansion (α) | 2.36*10−5 K−1 |
| Yield strength (σy) | 331 MPa | Specific heat capacity (c) | 714.8 J/kg*K |
| Unit elongation at break (ε) | 11% | 0.5% Fe, 0.4% Si, 1.2-2.0% Cu, 0.3% Mn, 2.1-2.9% Mg, 5.1-5.6% Zn, 0.18-0.28% Cr, 0.20% Ti, 0.15% Other, % Remaining Al | |
| Poisson's ratio (ν) | 0.33 | | |
| Degree of hardness | B 87/150 | | |

Aluminium (AA7075) alloy is one of the strongest aluminium alloys available, making it valuable in high-stress situations.

## 2.3 Cutting tool

In the drillability test carried out with the CNC Vertical Machining Centre Micron VCP 800, a total of 27 drillings were performed with three different drill types: nine drills with 15 µm corner rounding (Drill Type A), nine drills with 15 µm corner rounding and polishing (Drill Type B), nine drills with 25 µm corner rounding (Drill Type C) with tool dimensions of 5x41x82 mm. Fig. 6 shows the general view of the drill used in the drillability tests.

**Fig. 6** General view of the drill used in the drilling tests

**Table 3** Drill Properties

| Drill Type | Corner Rounding | Additional Process Applied |
|---|---|---|
| Type A | 15 µm | - |
| Type B | 15 µm | Polishing |
| Type C | 25 µm | - |

The material of the drill tool used in the drilling tests, whose specifications are shown in Table 3, and whose geometry is given in Fig. 6, is Tungsten Carbide Cobalt (WC-Co) alloy with an aluminium titanium nitride coating (AlTiN) on the drill. WC-Co is the most widely used high-speed machining drill tool material produced in powder metallurgy, consisting of hard metal particles and a softer metal bond. WC-Co tungsten carbide has the unique advantage of both rigidity and hardness. Nowadays, almost all WC-Co tools and bits are coated, and the modulus of elasticity of WC-Co is about three times that of high-speed steel. The type of aluminium titanium nitride coating, known as AlTiN, can reach processing temperatures as high as 800°C. WC is one of the most significant components used in the manufacture of tool materials [14].

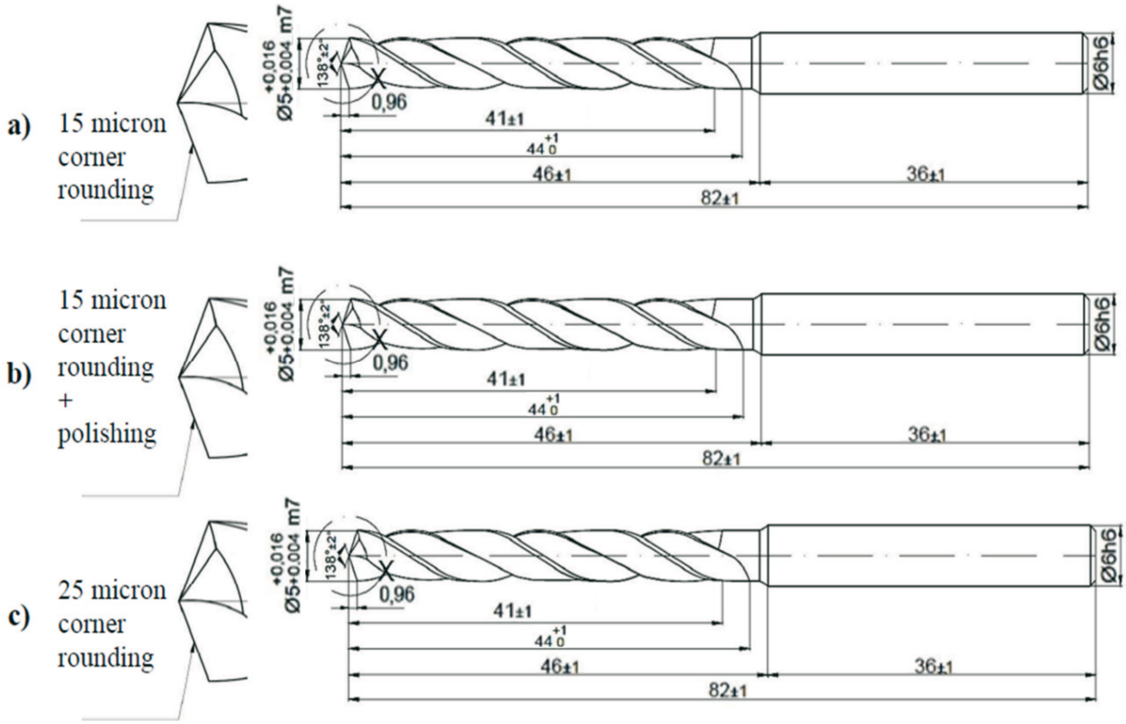


**Fig. 7** (a) Drill type A used in L1 to L9 drilling tests; (b) Drill type B used in L10 to L18 drilling tests; (c) Drill type C used in L19 to L27 drilling tests

## 2.4 Cutting force measurement

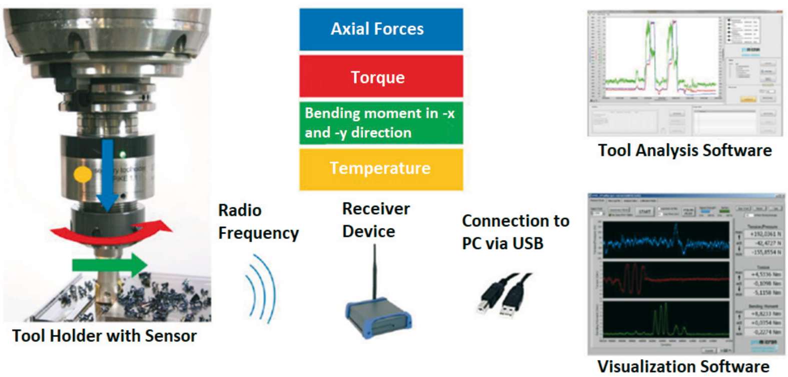


**Fig. 8** Data reading and transfer with mobile dynamometer


**Fig. 9** Force measurement dynamometer view

During the drilling test of the PAEK/CF and AA7075 stack, a mobile dynamometer (Spike® Mobile 1.2 Sensory Toolholder), which has a wireless receiver connection and is referred to as a smart tool and cutting force monitoring system, was used to measure the $Fz$ thrust force. The appearance of this system is presented in Fig. 8 and Fig. 9. This system senses the forces acting on the tool, the torsional moments, and the temperature of the measurement area during the cutting (drilling, milling) process, and these can be monitored throughout the process. The measured data are transmitted wirelessly to a computer and analysed in the relevant software environment, allowing optimisation of the cutting processes and tool control.

The sensory tool holder SPIKE® is a wireless force sensor used as a diagnosis tool or for tool monitoring. During machining (drilling or milling), it can measure the generated force and torque directly at the tool holder. The data can then be transmitted wirelessly to a receiver. SPIKE® can be utilised to optimise cutting and milling processes. The included PC software (SPIKE® BTKaBlue V 13.4 is used for the visualisation software) allows the user to measure and visualise the axial forces, torsion, and the resulting bending. The resulting raw data are stored in plain text file format (ASCII) and can be easily exported and used for analysis afterwards. A distinctive feature of the software is the depiction of measurement values in a polar diagram. In this diagram, the bending torque acting on the tool holder is shown as an angular function. Forces can thus be detected over the life of the tool, and even the forces on different cutting fluids can be detected. An integrated temperature sensor detects temperature at the place of the sensory ring and can therefore show the trends of the process temperature. For its mobile use, SPIKE® is powered via an integrated Li-Polymer rechargeable battery.

The filter frequency value used in the experiment is 1600 Hertz. The measurement rate without reduction amounts to about 1600 measurements per second, which adds up to about 6 MB per minute. The tool holder can only be activated via the built-in accelerometer. In the machine, the tool holder is automatically activated from a speed of about 300 rpm. Manually, the tool holder can be easily activated by spinning it by hand. After activation, measuring data are transmitted. If no acceleration is detected for one minute, the tool holder shuts down (a speed of <300 rpm). The reduction of the measured values is achieved by an averaging filter. At 160 measurements per second, only 10 measured values are identified, which reduces the amount of data by 90%.

## 2.5 Toolholder geometry

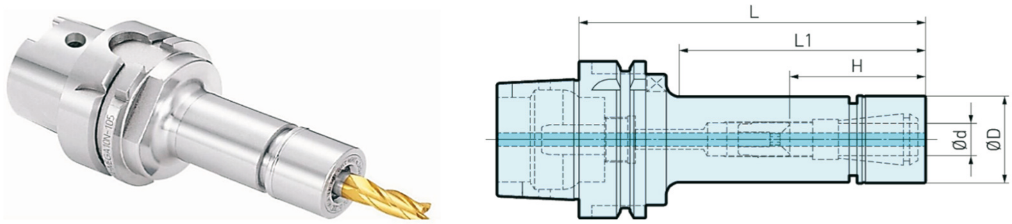


| ∅*d* | ∅*D* | *L* | *L1* | *H* |
|---|---|---|---|---|
| 2.5-20 | 46 | 105 | 69 | 51-54 |

**Fig. 10** HSK-A63-MEGA 20N-105 Toolholder geometry

The drillability experiment was conducted with the CNC Vertical Machining Centre Micron VCP 800, using the tool holder of model number HSK-A63-MEGA 20N-105, the geometry and dimensions of which are presented in Fig. 10.

## 2.6 Transferring data from the CNC Vertical Machining Centre Micron VCP 800 to the computer

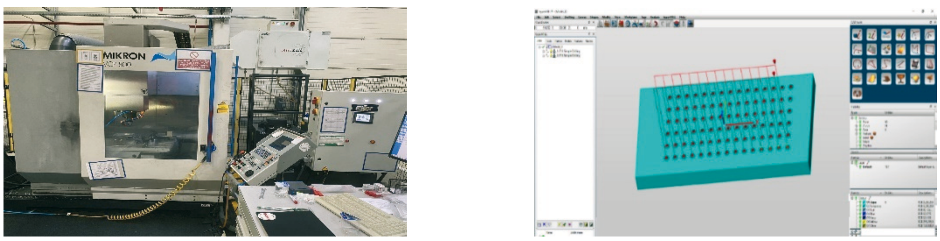

(a) (b)

**Fig. 11** (a) CNC Vertical Machining Centre Micron VCP 800; (b) *hyper*MILL® CAD/CAM Program

The values shown in Fig. 11(a) in the drillability test are as follows: X-axis movement: 800 mm; Y-axis movement: 600 mm; Z-axis movement: 500 mm; table length: 1050 mm; table width: 600 mm; maximum workpiece weight: 1100 kg; maximum spindle speed: 20,000 rpm; spindle motor power: 40 kW; length x width x height: 3160.0 × 2240.0 × 2645.0 mm; number of pots: 30 pieces; toolholder: HSK-A63, CNC Vertical Machining Centre Micron VCP 800, the view of which is presented in Fig. 12(a), with an air connection of 6 - 7 bar. The drillability tests were carried out by the stack drilling of thermoplastic matrix composite (Toray Cetex® TC1225) and aluminium (AA7075) materials, presented in Fig. 12(b), fixed to each other with bolted connections at four corners. The drilling dimensions of the composite-metal stack, the drilling process view of which is presented in Fig. 11, were designed and transferred to the CNC Vertical Machining Centre Micron VCP 800 with the hyperMILL® CAD/CAM program, a CAD/CAM solution used in milling and turning processes such as high-speed/high-performance cutting.

The numerical data, such as force, torque, etc., of the cutting tool were transferred to the computer by the Spike® Mobile 1.2 Sensory Toolholder dynamometer toolholder with SPIKE Tool Measurement 2016 SP3 EN Version 16.3.0.4 Promicron Wireless Solution software [15].

(a) (b)

**Fig. 12** (a) Pre-stack drilling view of the composite and AA7075 fixed on the CNC Vertical Machining Centre; (b) Post-stack drilling view of composite and AA7075

## 2.7 Tool wear measurement

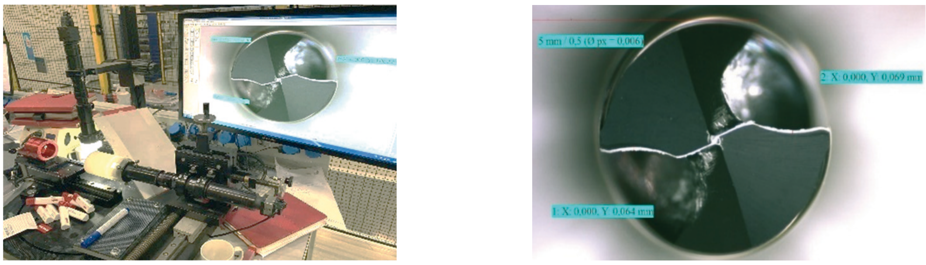

(a) (b)

**Fig. 13** (a) Tool wear measuring instrument; (b) Sample image of tool wear

The cutting tool damage measurement device, as shown in Fig. 13(a) and Fig. 13(b), was produced by the company where the drillability test was carried out. The cutting tool damage can be measured at the micron level with the Metric 9.00 MT software produced by M-Service & Geräte. The tool wear parameters are drill type (A, B, C), cutting speed (55 m/min, 95 m/min, 165 m/min) and feed rate (0.1 mm/rev, 0.2 mm/rev, 0.3 mm/rev). The drillability tests used 15 µm corner rounding (Drill Type A), 15 µm corner rounding and polishing (Drill Type B), 25 µm corner rounding (Drill Type C) with tool dimensions of 5x41x82 mm.

## 2.8 Composite material hole entry and exit morphology and hole damage

Fig. 14(a) shows the optical microscope image of the thermoplastic matrix composite material hole entrance from the top. Fig. 14(b) shows the bottom hole exit after the drilling test. Hole damage is visible, especially in the exit holes.

**(a)** **(b)**

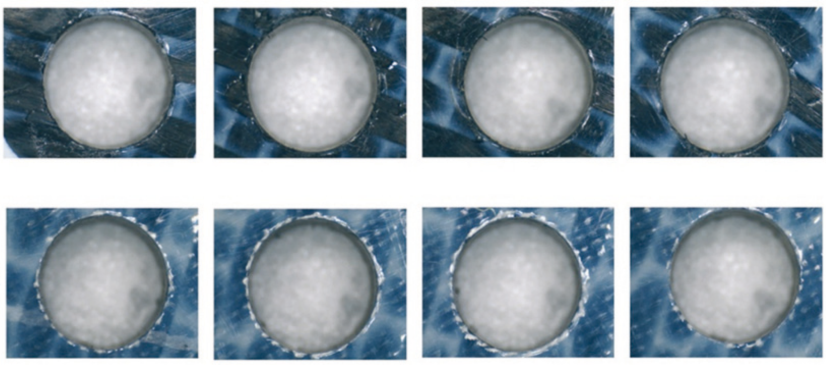

**Fig. 14** (a) Hole entrance, (b) Hole exit

## 3. Experiment design

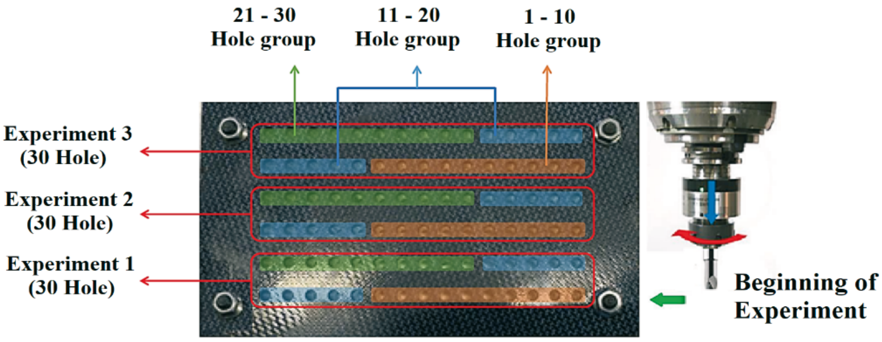


**Fig. 15** Experiment layout

The experimental drilling arrangement is illustrated in Fig. 15. For the drillability tests, 810 holes were drilled in total, 30 holes for each of the 27 drillability tests on the samples fixed to each other as shown in Fig. 14, with the PEEK/CF (Polyether Ether Ketone) thermoplastic matrix composite from the Poly Aryl Ether Ketone (PAEK) family and aluminium (AA7075) stack structure. The combination of the experimental parameters A, B, and C drill types, V*c* cutting speed (m/min), and *f* feed rate (mm/rev) in Table 3 results in V*B* tool wear (mm) values. Numerical data on tool wear values and the applied force recorded at each stage of the 27 experiments with 30 holes each were collected and analysed with Minitab® 21.1 statistical software. Table 3 shows the drill types A, B, and C used in the experiment, cutting speed (V*c*) m/min, and feed rate (*f*) mm/rev. For each experiment, the maximum tool wear value of the drill cutting edges in the process of drilling 30 holes for each experiment was determined, and the values are presented in Table 4.

**Table 4** Test parameters and tool wear values

| Experiment No | Drill Type (A, B, C) | *(Vc)* Cutting Speed /(m/min) | *(f)* Feed Rate /(mm/rev) | *(VB)* Tool Wear /mm |
|---|---|---|---|---|
| **Experiment 1** | A | 55 | 0.1 | 0.069 |
| **Experiment 2** | A | 55 | 0.2 | 0.069 |
| **Experiment 3** | A | 55 | 0.3 | 0.052 |
| **Experiment 4** | A | 95 | 0.1 | 0.064 |
| **Experiment 5** | A | 95 | 0.2 | 0.069 |
| **Experiment 6** | A | 95 | 0.3 | 0.046 |
| **Experiment 7** | A | 165 | 0.1 | 0.069 |
| **Experiment 8** | A | 165 | 0.2 | 0.069 |
| **Experiment 9** | A | 165 | 0.3 | 0.040 |
| **Experiment 10** | B | 55 | 0.1 | 0.040 |
| **Experiment 11** | B | 55 | 0.2 | 0.040 |
| **Experiment 12** | B | 55 | 0.3 | 0.046 |
| **Experiment 13** | B | 95 | 0.1 | 0.052 |
| **Experiment 14** | B | 95 | 0.2 | 0.052 |
| **Experiment 15** | B | 95 | 0.3 | 0.046 |
| **Experiment 16** | B | 165 | 0.1 | 0.064 |
| **Experiment 17** | B | 165 | 0.2 | 0.035 |
| **Experiment 18** | B | 165 | 0.3 | 0.035 |
| **Experiment 19** | C | 55 | 0.1 | 0.075 |
| **Experiment 20** | C | 55 | 0.2 | 0.035 |
| **Experiment 21** | C | 55 | 0.3 | 0.029 |
| **Experiment 22** | C | 95 | 0.1 | 0.116 |
| **Experiment 23** | C | 95 | 0.2 | 0.040 |
| **Experiment 24** | C | 95 | 0.3 | 0.023 |
| **Experiment 25** | C | 165 | 0.1 | 0.087 |
| **Experiment 26** | C | 165 | 0.2 | 0.075 |
| **Experiment 27** | C | 165 | 0.3 | 0.046 |

## 4. Results and discussion

The cutting force and tool wear values in the first 10 hole groups of 270 holes were evaluated by an analysis of variance using the Minitab® 21.1 Statistical Software program, and the results are presented in Table 5.

### 4.1 Evaluation of drilling test with an analysis of variance for the first 10 hole groups

**Table 5** Analysis of variance (ANOVA) of holes 1 – 10

| Source of Variance | Degrees of Freedom (DOF) | Total Sum of Squares (TSS) | Mean Squares (MS) | F-Value | P-Value | Percentage Effect (%) |
|---|---|---|---|---|---|---|
| Model | 35 | 8946237 | 255607 | 127.55 | 0 | 95.02 |
| Blocks | 9 | 212038 | 23560 | 11.76 | 0 | 2.25 |
| Linear | 6 | 4939385 | 823231 | 410.8 | 0 | 52.46 |
| Drill Type | 2 | 808434 | 404217 | 201.71 | 0 | 8.59 |
| Cutting Speed | 2 | 1535270 | 767635 | 383.06 | 0 | 16.31 |
| Feed Rate | 2 | 2595681 | 1297841 | 647.64 | 0 | 27.57 |
| Two-Way Interactions | 12 | 1842849 | 153571 | 76.63 | 0 | 19.57 |
| Drill Type*Cutting Speed | 4 | 780419 | 195105 | 97.36 | 0 | 8.29 |
| Drill Type*Feed Rate | 4 | 901007 | 225252 | 112.4 | 0 | 9.57 |
| Cutting Speed*Feed Rate | 4 | 161424 | 40356 | 20.14 | 0 | 1.71 |
| Three-Way Interactions | 8 | 1951965 | 243996 | 121.76 | 0 | 20.73 |
| Drill Type*Cutting Speed*Feed Rate | 8 | 1951965 | 243996 | 121.76 | 0 | 20.73 |
| Error | 234 | 468928 | 2004 | | | 4.98 |
| Total | 269 | 9415165 | | | | 100.00 |

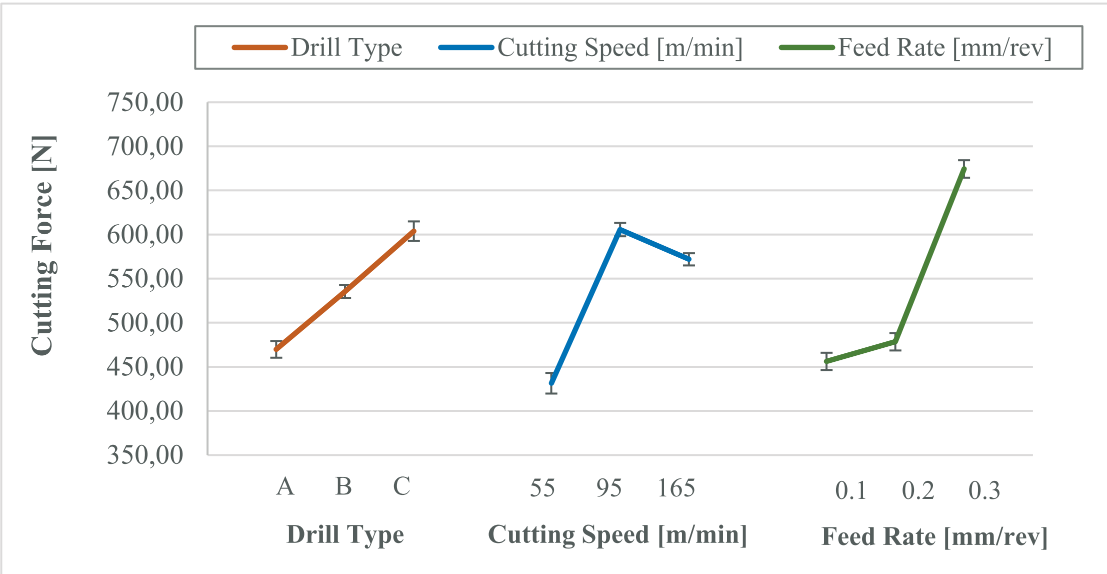


**Fig. 16** Effect of cutting parameters on the cutting forces in holes 1 – 10

For the first 10 hole groups (holes 1-10) in which 270 holes were drilled, the analysis of variance (ANOVA) of holes 1-10 is shown in Table 5, and the evaluation of the effect of the cutting parameters on the cutting forces in holes 1-10 is shown in Fig. 16.

- In terms of cutting force, the most effective cutting parameter based on the percentage effect ratio in the first 10 holes was found to be a feed rate with a percentage effect of 27.57% in the 1st rank, a cutting speed with a percentage effect of 16.31% in the 2nd rank, and drill type with a percentage effect of 8.59% in the 3rd rank.
- In terms of drill type, it was determined that in holes 1-10, the drill type A drilled holes with the lowest cutting force, and the drill type C drilled holes with the highest cutting force.

- In terms of cutting speed, for holes 1-10, the lowest cutting force occurred at a cutting speed of 55 m/min, and the highest cutting force occurred at a cutting speed of 95 m/min.
- In terms of feed rate, the lowest cutting force in holes 1-10 was obtained with a feed rate of 0.1 mm/rev, and the highest cutting force was obtained with a feed rate of 0.3 mm/rev.

## 4.2 Evaluation of drilling tests with an analysis of variance for the second 10-hole group

**Table 6** Analysis of variance (ANOVA) of holes 11 – 20

| Source of Variance | Degrees of Freedom (DOF) | Total Sum of Squares (TSS) | Mean Squares (MS) | F-Value | P-Value | Percentage Effect (%) |
|---|---|---|---|---|---|---|
| Model | 35 | 7682647 | 219504 | 41.52 | 0 | 86.13 |
| Blocks | 9 | 49068 | 5452 | 1.03 | 0.416 | 0.55 |
| Linear | 6 | 4126012 | 687669 | 130.08 | 0 | 46.26 |
| Drill Type | 2 | 1548832 | 774416 | 146.49 | 0 | 17.36 |
| Cutting Speed | 2 | 1073548 | 536774 | 101.54 | 0 | 12.04 |
| Feed Rate | 2 | 1503632 | 751816 | 142.22 | 0 | 16.86 |
| Two-Way Interactions | 12 | 1384713 | 115393 | 21.83 | 0 | 15.52 |
| Drill Type*Cutting Speed | 4 | 401101 | 100275 | 18.97 | 0 | 4.50 |
| Drill Type*Feed Rate | 4 | 792620 | 198155 | 37.48 | 0 | 8.89 |
| Cutting Speed*Feed Rate | 4 | 190991 | 47748 | 9.03 | 0 | 2.14 |
| Three-Way Interactions | 8 | 2122854 | 265357 | 50.2 | 0 | 23.80 |
| Drill Type*Cutting Speed*Feed Rate | 8 | 2122854 | 265357 | 50.2 | 0 | 23.80 |
| Error | 234 | 1237013 | 5286 | | | 13.87 |
| Total | 269 | 8919660 | | | | 100.00 |

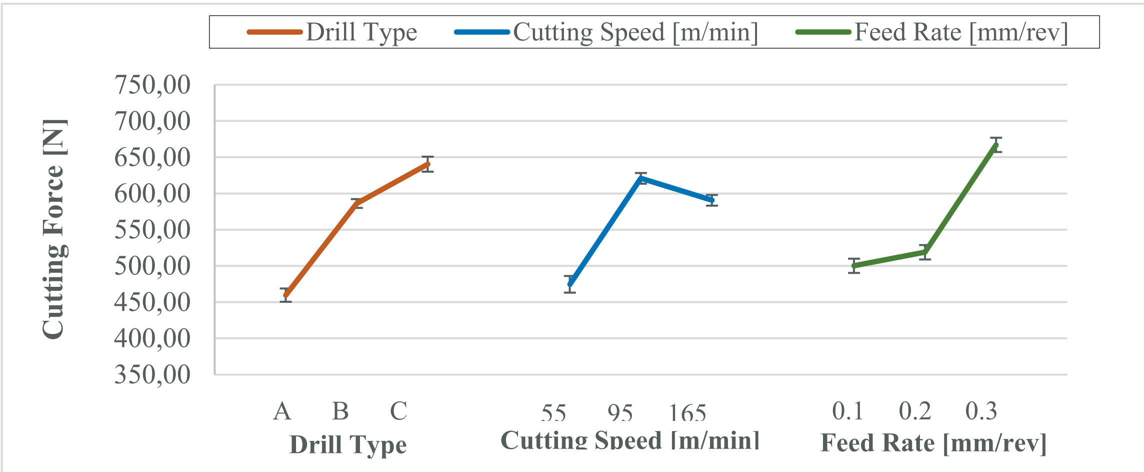


**Fig. 17** Effect of cutting parameters on cutting forces in holes 11 – 20

For the second 10-hole group (holes 11-20) in which 270 holes were drilled, the analysis of variance (ANOVA) of holes 11 – 20 is shown in Table 6, and the evaluation of the effect of the cutting parameters on the cutting forces in holes 11 – 20 is shown in Fig. 17.

- In terms of cutting force, the most effective cutting parameter based on the percentage effect ratio in the second 10 holes was found to be a drill type with a percentage effect of 17.36% in the 1st rank, a feed rate with a percentage effect of 16.86% in the 2nd rank, and a cutting speed with a percentage effect of 12.04% in the 3rd rank.
- In terms of drill type, it was determined that in holes 11-20, drill type A drilled holes with the lowest cutting force, and drill type C drilled holes with the highest cutting force.
- In terms of cutting speed, the lowest cutting force occurred at 55 m/min for holes 11 and 20, and the highest at 95 m/min.

- In terms of feed rate, the lowest cutting force in holes 11-20 was obtained with a feed rate of 0.1 mm/rev, and the highest cutting force was obtained with a feed rate of 0.3 mm/rev.

## 4.3 Evaluation of drilling tests with an analysis of variance for the third 10-hole group

**Table 7** Analysis of Variance (ANOVA) of holes 21 – 30

| Source of Variance | Degrees of Freedom (DOF) | Total Sum of Squares (TSS) | Mean Squares (MS) | F-Value | P-Value | Percentage Effect (%) |
|---|---|---|---|---|---|---|
| Model | 35 | 8763884 | 250397 | 143.31 | 0 | 95.54 |
| Blocks | 9 | 26223 | 2914 | 1.67 | 0.098 | 0.29 |
| Linear | 6 | 3872147 | 645358 | 369.35 | 0 | 42.21 |
| Drill Type | 2 | 2255474 | 1127737 | 645.43 | 0 | 24.59 |
| Cutting Speed | 2 | 766652 | 383326 | 219.39 | 0 | 8.36 |
| Feed Rate | 2 | 850020 | 425010 | 243.24 | 0 | 9.27 |
| Two-Way Interactions | 12 | 2100154 | 175013 | 100.16 | 0 | 22.90 |
| Drill Type*Cutting Speed | 4 | 328684 | 82171 | 47.03 | 0 | 3.58 |
| Drill Type*Feed Rate | 4 | 1362125 | 340531 | 194.89 | 0 | 14.85 |
| Cutting Speed*Feed Rate | 4 | 409344 | 102336 | 58.57 | 0 | 4.46 |
| Three-Way Interactions | 8 | 2765361 | 345670 | 197.84 | 0 | 30.15 |
| Drill Type*Cutting Speed*Feed Rate | 8 | 2765361 | 345670 | 197.84 | 0 | 30.15 |
| Error | 234 | 408860 | 1747 | | | 4.46 |
| Total | 269 | 9172744 | | | | 100.00 |

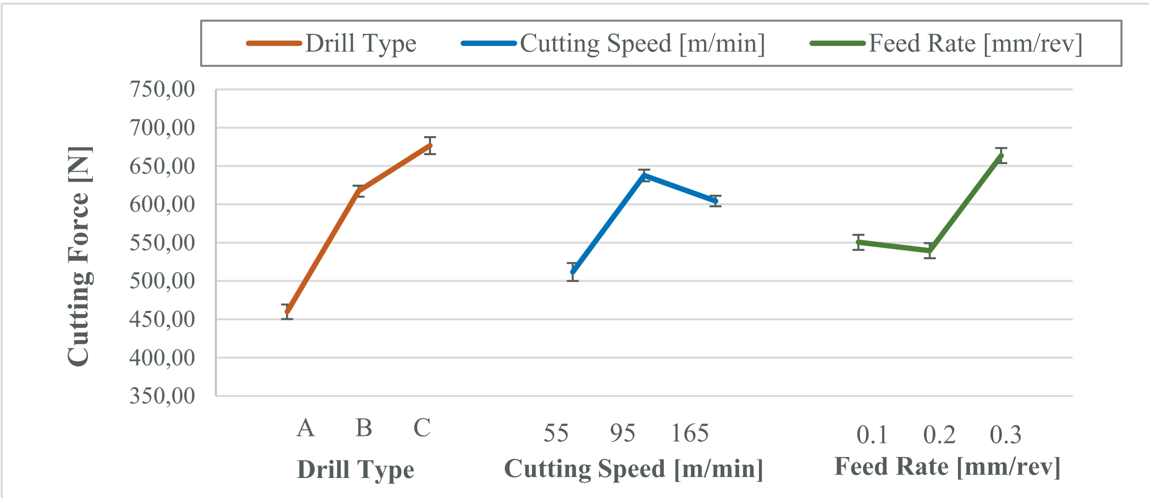


**Fig. 18** Effect of cutting parameters on cutting forces in holes 21 – 30

For the third 10-hole group (holes 21-30) in which 270 holes were drilled, the analysis of variance (ANOVA) of holes 21 – 30 is shown in Table 7, and the evaluation of the effect of the cutting parameters on the cutting forces in holes 21 – 30 is shown in Fig. 18.

- In terms of cutting force, the most effective cutting parameter based on the percentage effect ratio in the third group of 10 holes was found to be a drill type with a percentage effect of 24.59% in the 1st rank, a feed rate with a percentage effect of 9.27% in the 2nd rank, and a cutting speed with a percentage effect of 8.36% in the 3rd rank.
- In terms of drill type, it was determined that in holes 21-30, drill type A drilled holes with the lowest cutting force, and drill type C drilled holes with the highest cutting force.
- In terms of cutting speed, for holes 21-30, the lowest cutting force occurred at a cutting speed of 55 m/min, and the highest cutting force occurred at a cutting speed of 95 m/min.
- In terms of feed rate, the lowest cutting force in holes 21-30 was obtained with a feed rate of 0.2 mm/rev, and the highest cutting force was obtained with a feed rate of 0.3 mm/rev.

## 4.4 Analysis of variance to evaluate the effect of drill type, cutting speed, and feed rate on tool wear

**Table 8** Analysis of variance for tool wear

| Source of Variance | Degrees of Freedom (DOF) | Total Sum of Squares (TSS) | Mean Squares (MS) | F-Value | P-Value | Percentage Effect (%) |
|---|---|---|---|---|---|---|
| Model | 18 | 0.009412 | 0.000523 | 2.93 | 0.062 | 86.8 |
| Linear | 6 | 0.005634 | 0.000939 | 5.27 | 0.018 | 52.0 |
| Drill Type | 2 | 0.00121 | 0.000605 | 3.39 | 0.086 | 11.2 |
| Cutting Speed | 2 | 0.000266 | 0.000133 | 0.75 | 0.505 | 2.5 |
| Feed Rate | 2 | 0.004158 | 0.002079 | 11.67 | 0.004 | 38.4 |
| Two-Way Interactions | 12 | 0.003778 | 0.000315 | 1.77 | 0.213 | 34.9 |
| Drill Type*Cutting Speed | 4 | 0.000663 | 0.000166 | 0.93 | 0.492 | 6.1 |
| Drill Type*Feed Rate | 4 | 0.002736 | 0.000684 | 3.84 | 0.05 | 25.2 |
| Cutting Speed*Feed Rate | 4 | 0.000378 | 0.000095 | 0.53 | 0.717 | 3.5 |
| Error | 8 | 0.001426 | 0.000178 | | | 13.2 |
| Total | 26 | 0.010838 | | | | 100 |

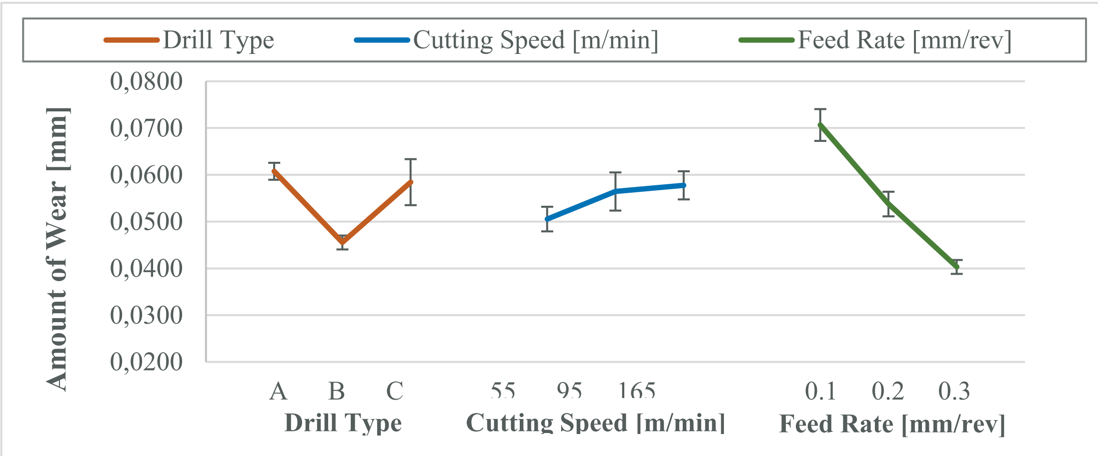


**Fig. 19** Variation of tool wear with drill type, cutting speed, and feed rate

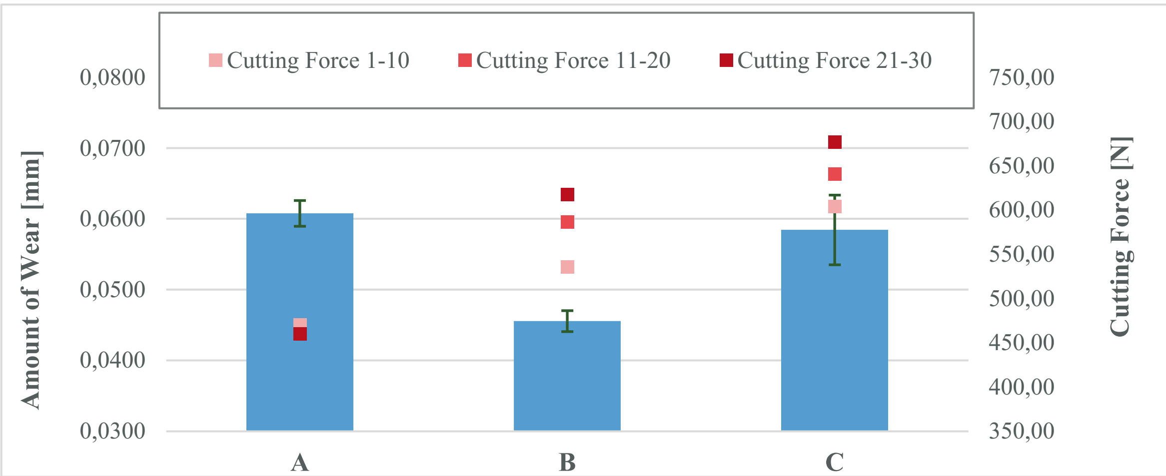


**Fig. 20** Tool wear of drill types A, B, and C, according to cutting forces

Overall, 810 holes were drilled in the experiment, and an analysis of variance was performed to evaluate the effect of the drill type, cutting speed, and feed rate on tool wear. The results are presented in Table 8. The tool wear of drill types A, B, and C according to the cutting forces was analysed, and the results are presented in Fig 20. The analysis yielded the following results.

- In terms of tool wear, the most effective cutting parameter based on the percentage effect ratio in the whole experimental process was found to be a feed rate with a percentage effect of 38.4% in the 1st rank, drill type with a percentage effect of 11.2% in the 2nd rank, and a cutting speed with a percentage effect of 2.5% in the 3rd rank.
- It was determined that the lowest tool wear among drill types A, B, and C was the type B drill that was subjected to polishing. In other words, the polishing process reduced tool wear. It was found that the highest level of tool wear was in the type A drill, which, compared to drill type C, had less cutting edge rounding and was subjected to more wear, while drill type C with less edge rounding than drill type A was subjected to less tool wear than the type A drill.
- Throughout the experiment, it was found that tool wear increased with higher cutting speeds.

## 4.5 Discussion

A comparison of this study with the literature review provides the following insights within the framework of the analysis of our experimental study: in terms of cutting force, the most effective cutting parameter based on the percentage effect ratio in the first 10 holes was found to be a feed rate with a percentage effect of 27.57% in the 1st rank, a cutting speed with 16.31% in the 2nd rank, and drill type with 8.59% in the 3rd rank, as can be seen in Table 5 and Fig. 16. In terms of tool wear, the most effective cutting parameter based on the percentage effect ratio graph in the whole experimental process was found to be a feed rate with a percentage effect of 38.4% in the 1st rank, drill type with 11.2% in the 2nd rank, and cutting speed with 2.5% in the 3rd rank, as presented in Table 8. In the article by Davim and Reis [16], the experiments showed that the feed rate is the cutting parameter that has the highest physical and statistical influence on the cutting force. On the same basis, Eneyew and Ramulu [17] concluded that the cutting force is affected by the feed rate more than the cutting speed and this result is consistent with the result obtained by an analysis of variance in our study by the data of drilling tests given in Fig. 19 and Fig. 20. In another study by Geier and Szalay [18], the ANOVA results and main effect plots show that the feed rate has the most significant effect on the cutting force, consistent with the data obtained from our drilling experiments. In another study, Hwan, Ge and Song [23] observed that the cutting force increases as the number of holes increases, and in our experimental study, in line with Hwan, Ge and Song, and as can be observed in Fig. 20, it is determined that in the hole groups 1-10, 11-20 and 21-30, the cutting force rises as the number of holes increases.

- A comparison of this study with the literature research shows that in our experimental study, as can be inferred from Fig. 20, which shows the tool wear of tool types A, B, and C for cutting forces, it was determined that raising the cutting speed increases the tool wear. In the literature, research conducted by Goutham, Mathew and Vijayaraghavan [19] found that the cutting force increases significantly with the increase in the number of holes, and this overlaps exactly with the experimental results in our study. In the study conducted by Lin and Chen [20] with the same principles, it was found that the cutting force increased due to tool wear as the drilling amount/distance increased, and that study also supports our experimental study. In the experimental study conducted by Zhanget al [22], it was found that the cutting force increases gradually from the first hole, which could be due to the rapid wear of the cutting edge of the new tool in the early stage of the drilling process. In our study, as can be concluded from Fig. 19, it is evident that the increase in the cutting force increases the tool wear, and the results we obtained are in line with the aforementioned study.
- In our drilling study, tool wear and cutting forces are compared in Fig. 20. The table in question shows that tool wear increases with the increase in the cutting speed throughout the experiment. Based on the research in the literature, Jagadeesh et al [21] conducted experimental studies and found that the increase in cutting forces causes tool wear. The experimental research of Lin and Chen [20] indicates that tool wear increases as the

cutting speed grows, consistent with the results of our study. The difference in our study is that in the tool wear graphs of drill types A, B and C shown in Fig. 20, it can be seen that even though the cutting forces of drill type B increase, the tool wear is lower than that of drill types A and C, which is considered to be due to the easy removal of the chip as a result of the polishing process in drill type B.

## 5. Conclusion

The following results were obtained as a result of the investigation of the effect of the cutting parameters on the cutting forces and tool wear in the stacked drilling of a carbon fibre-reinforced thermoplastic matrix composite and AA7075.

- The feed rate was found to have the highest physical and statistical effect on the cutting forces and tool wear among the cutting parameters.
- When the hole groups were analysed, it was observed that the cutting force increases as the number of drilled holes increases, and this is related to tool wear. As a positive result of the polishing process applied to drill type B, it was determined that even if the cutting force increases, the tool wear is lower when compared to drill types A and C.
- Throughout the experiment, it was found that tool wear increases with the increasing cutting speed.
- Due to the reduction in friction in the polished drill type, tool wear and heating are reduced and chip output speeds up. It seems that the increase in cutting speed has a positive effect on the completion time of the drilling process, and the tool life has a positive effect on the total cost. An in-depth analysis of the evolution of tool geometry, cutting forces, the feed rate and tool wear has allowed us to achieve these experimental results.

## Acknowledgments

The authors sincerely thank Karcan Cutting Tool Industry and Trade Inc. for providing the cutting tools, experiments and measurements in this study.

## REFERENCES

[1] Baş O., Ateş E., Öztürk F., **2021**. Thermoplastic Composite Materials for the Aerospace Industry, Crimson Publishers, Volume 15 - Issue 5. https://doi.org/10.31031/RDMS.2021.15.000872

[2] Thomasnet, «A Brief History of Aircraft Materials» 17 08 **2023**. [Çevrimiçi]. Available : https://www.thomasnet.com/insights/a-brief-history-of-aircraft-materials/#

[3] Birley, A. W., Heath, R. J., & Scoot, M. J., **1994**. Plastic Materials: Properties and Applications 2nd Edition. Blackie Academic and Professional.

[4] Margolis, J. M., **2020**. Engineering Thermoplastics: Properties and Applications. CRC Press. https://doi.org/10.1201/9781003066156

[5] Usama A. Khashaba, Mohamed S. Abd Elwahed, Mohamed, A. Eltaher, Ismail Najjar, Ammar Melaibari, Khaled I. Ahmed, 2021, Thermo-Mechanical and Delamination Properties In Drilling GFRP Composıtes By Varıous Drill Angles, Polymers - an Open Access Journal by MDPI, 13 (11) – 1884. https://doi.org/10.3390/polym13111884

[6] Zhang, L., Wang, X., Pei, J., Zhou, Y.,2020, Review Of Automated Fibre Placement And İts Prospects For Advanced Composites, J Mater Sci., **2020** 55:7121–7155. https://doi.org/10.1007/s10853-019-04090-7

[7] Northrop Grumman, «Aerospace Structures Overview» 02 09 **2023** [Çevrimiçi]. Available: https://wpcontent.ot5o9s93syrb.net/wp-content/uploads/Northrop-Grumman-Aerospace-Structures.pdf#

[8] Flight Global, «The future of aerospace is plastics?» 03 09 **2023** [Çevrimiçi], Available: https://www.flightglobal.com/paid-content/the-future-of-aerospace-isplastics/147262.article /#

[9] Franke, V., **2011**, " Drilling of long fiber reinforced thermoplastics - Influence of the cutting edge on the machining results", CIRP Annals - Manufacturing Technology 60 : pp 65–68. https://doi.org/10.1016/j.cirp.2011.03.078

[10] Toray Advanced Composites Product Data Sheet «Toray Cetex® 1225» 24 08 **2023** [Çevrimiçi]. Avilable: https://www.toraytac.com/product-explorer/products/gXuK/Toray Cetex-TC1225/#.

[11] M. Holmes, «Aerospace Looks To Composites For Solutions» Elsevier, Reinforced Plastics, **2017** Volume 61, Number 4. https://doi.org/10.1016/j.repl.2017.06.079

[12] EN AW 7075 Alüminyum Özellikleri «Havacılık ve Uzay Sanayi» 10 09 **2023** [Çevrimiçi] Available: https://aluminyumburada.com/blog?p=en-aw-7075-aluminyum-ozellikler

[13] 7075 Alüminyum - Özellikleri, Mukavemeti ve Kullanım Alanları 11 09 2023 [Çevrimiçi], Available: https://tr.czyzindustry.com/info/7075-aluminum-properties-strength-and-uses-58088101.html

[14] Oruç, Ö. **2006** Termoreaktif Difüzyon Tekniği ile Borlanmıs Wc-Co Esaslı Kesici Takımların Karekterizasyonu ve Aşınma Davranışının İncelenmesi, Yüksek Lisans Tezi, S.Ü.F.B.E, İstanbul, Türkiye, Syf. 30

[15] Promicron Wireless Solution, **2015**. SPIKE® Sensory Tool Holder User Manual Sensory Tool Holder SPIKE, (2015), Pro-Micron GmbH & Co. KG Innovapark 20 87600 Kaufbeuren

[16] Davim, J., Reis, P., **2003**. Drilling carbon fiber reinforced plastics manufactured by autoclave experimental and statistical study. Materials and Design 24 (2003) 315-324. https://doi.org/10.1016/S0261-3069(03)00062-1

[17] Eneyew,E., Ramulu M., **2014**. Experimental study of surface quality and damage when drilling unidirectional CFRP composites, Journal of Materials Research and Technology, 2014;3(4):354-362. https://doi.org/10.1016/j.jmrt.2014.10.003

[18] Geier, N., Szalay T., **2017**. Optimisation of process parameters for the orbital and conventional drilling of uni-directional carbon fibre-reinforced polymers (UD-CFRP). Measurement, 110 (2017) 319–334. https://doi.org/10.1016/j.measurement.2017.07.007

[19] Goutham, K., Mathew, N., Vijayaraghavan L., **2022**. Delamination and tool wear in drilling of carbon fabric reinforced epoxy composite laminate. Materials Today: Proceedings 50 (**2022**) 823–829. https://doi.org/10.1016/j.matpr.2021.06.030

[20] Lin,S., Chen, I., **1996**. Drilling carbon fiber-reinforced composite material at high speed. Wear 194 (1996) 156-162. https://doi.org/10.1016/0043-1648(95)06831-7

[21] Jagadeesh, P., Rangappa, M., Suyambulingam, I., Siengchin, S., Puttegowda, M., Binoj, J., Gorbatyuk, S., Khan, A., Doddamani, M., Fiore, V., Cuadrado, M., **2023**. Drilling characteristics and properties analysis of fiber reinforced polymer composites: A comprehensive review. Heliyon 9, **2023**. https://doi.org/10.1016/j.heliyon.2023.e14428

[22] Zhang, B., Sui, T.,Lin, B., Zheng, W., Li, S., Fang, S.,Huang, Y., Feng Y., **2022**. Drilling process of Cf/SiC ceramic matrix composites: Cutting force modeling, machining quality and PCD tool wear analysis. Journal of Materials Processing Tech. 304 (2022). https://doi.org/10.1016/j.jmatprotec.2022.117566

[23] Hwan, J., Ge, J., Song, J., **2021**. Study on Burr Formation and Tool Wear in Drilling CFRP and Its Hybrid Composites, Applied Sciences, 2021, 11, 384. https://doi.org/10.3390/app11010384

Submitted: 28.02.2024
Accepted: 15.10.2024

Ali Coşkun*
PhD student
Marmara University, Institute of Pure and Applied Science, Mechanical Engineering Department, Istanbul, Turkey

Assoc. Prof. Dr. Ayhan Etyemez
Prof. Dr. Mustafa Ay
Prof. Dr. Mustafa Kurt
Marmara University, Mechanical Engineering Department, Istanbul, Turkey

Dr. Şükran Katmer
Prof. Dr. Ulvi Şeker
Gazi University, Manufacturing Engineering Department, Ankara, Turkey

Mrs. Mine Nohuz
İzmir Institute of Technology, Materials Science and Engineering, Güzelbahçe Campus, Urla-İzmir, Turkey

*Corresponding author:
ali.coskun@marun.edu.tr